

UDC 532: [612.1+616.1]  
DOI: 10.21668/health.risk/2022.4.15.eng

Read  
online 

Research article

## PATIENT-SPECIFIC 0D-3D MODELING OF BLOOD FLOW IN NEWBORNS TO PREDICT RISKS OF COMPLICATIONS AFTER SURGERY

**A.G. Kuchumov<sup>1</sup>, M.R. Kamaltdinov<sup>2</sup>, A.R. Khairulin<sup>1</sup>, M.V. Kochergin<sup>1</sup>, M.I. Shmurak<sup>1</sup>**

<sup>1</sup>Perm National Research Polytechnic University, 29 Komsomolskii Ave., Perm, 614990, Russian Federation

<sup>2</sup>Federal Scientific Center for Medical and Preventive Health Risk Management Technologies, 82 Monastyrskaya Str., Perm, 614045, Russian Federation

*Abnormal developments of the cardiovascular system are common congenital malformations. Computational fluid dynamics and mathematical modeling can be used to perform quantitative predictive assessments of hemodynamic properties in varied conditions.*

*This article addresses the development of a coupled 0D-3D model of blood flow in newborns to predict risks of complications after surgery. The 0D-model of systemic circulations is created by using the analogy between the blood flow in vessels and the flow of current through an electric circuit. A shunted section of the aorta and pulmonary artery is replaced with a 3D-model with two-way fluid-solid interaction (FSI). A section in a vessel with the aortic valve is examined in a separate 3D-model. Three-dimensional geometry is based on real CT-scans of a patient. The algorithm for coupling models of different levels relies on meeting the condition that pressures and volumetric blood flows are equal at the interaction boundary.*

*We have developed an algorithm for identifying personal parameters from the results obtained by solving an optimization problem. Computational experiments with different individual geometry of the aorta and aortic valve made it possible to analyze blood flow velocities, near-wall stresses, flows, and valve deformations. Observable near-wall stresses can be considered risk factors that could cause calcification on valve leaflets and other valve diseases.*

*Computational solutions in the “aorta – shunt – pulmonary artery” 3D-system allowed obtaining spatial distributions of velocities, pressures, near-wall stresses and other parameters that are significant in respect to probable pathology development. The developed approaches are primarily relevant for decision-making in surgical practice to predict risks of postoperative complications. In future, our plans are to develop the model so that it covers also saturation and oxygen exchange. This is necessary for assessing whether oxygen supply to the lungs is adequate.*

**Keywords:** 0D-3D model of blood flow, coupling algorithm, identification of parameters, patient-oriented, aorta, heart valve, newborn, shunt, risk of postoperative complications.

Obstructive lesions of the right ventricular outflow tract, both isolated and combined with other congenital heart diseases, account for 25–30 % of all congenital malformations of the heart [1]. When an inter-system shunt was first introduced (in particular, a modified Blalock – Taussig shunt), it became a real

breakthrough in surgical treatment of cyanotic heart diseases such as Tetralogy of Fallot, pulmonary atresia and some others [2, 3]. It is noteworthy that the modified Blalock – Taussig shunt remains a risky procedure that may result in extreme volume loads and acute thrombosis [4, 5]. To select an optimal shunt

© Kuchumov A.G., Kamaltdinov M.R., Khairulin A.R., Kochergin M.V., Shmurak M.I., 2022

**Alex G. Kuchumov** – Doctor of Physical and Mathematical Sciences, Associate Professor of Computational Mathematics, Mechanics and Biomechanics Department (e-mail: kychymov@inbox.ru; tel.: +7 (342) 239-15-64; ORCID: <https://orcid.org/0000-0002-0466-175X>).

**Marat R. Kamaltdinov** – Candidate of Physical and Mathematical Sciences, Head of the Situation Modeling and Expert and Analytical Management Techniques Laboratory (e-mail: kmr@fcrisk.ru; tel.: +7 (342) 237-18-04; ORCID: <http://orcid.org/0000-0003-0969-9252>).

**Alexander R. Khairulin** – student of Computational Mathematics, Mechanics and Biomechanics Department (e-mail: s.xayrulin@mail.ru; tel.: +7 (342) 239-17-02; ORCID: <https://orcid.org/0000-0002-7506-5568>).

**Maxim V. Kochergin** – student of Computational Mathematics, Mechanics and Biomechanics Department (e-mail: breakingkeyboard@gmail.com; tel.: +7 (342) 239-17-02).

**Marina I. Shmurak** – Candidate of Physical and Mathematical Sciences, Associate Professor of Computational Mathematics, Mechanics and Biomechanics Department (e-mail: shmurak2007@yandex.ru; tel.: +7 (342) 239-17-02; ORCID: <https://orcid.org/0000-0001-8060-7643>).

size is a vital task that hasn't been solved so far [6, 7].

Aortic valve disease is a most widely spread cardiovascular pathology. Valve disorders can be congenital when a valve with two leaflets is formed; or they can develop later when the valve leaflets become calcified [8, 9]. Valve disease is usually diagnosed by a physician who examines electrocardiography images of a specific patient and this estimation is rather subjective [10]. Exact methods are needed in this area since they allow quantitative assessments of functions performed by the aortic valve. Computer modeling makes it possible to simulate the aortic valve motion with precision and to obtain relevant data that are necessary for qualitative and quantitative assessment of the valve functioning [11].

Combined use of computational hydrodynamics and mathematical modeling has several advantages. First, we can predict blood flow properties under varied scenarios of surgery. Second, modeling results allow identifying critical health parameters of a specific patient that can be used as an indication to consider whether a surgery is advisable or not. Besides, biomechanical modeling can predict certain fundamental regularities that are typical for pathological processes.

At present, there is common understanding that it is necessary to develop complex multi-scale models to solve such tasks [12]. Experts have created basic principles for 0D, 1D, 3D coupling to identify blood flow properties [13, 14]. The study [15] addressed coupling of 1D – 3D models with vascular walls rigidity considered in the process. The authors of the study [16] coupled a finite-element model of the aorta and left ventricle and a 0D-circulation model for a patient with diagnosed pulmonary arterial hypertension. The study [17] concentrated on properties of coupled 3D-solid state two-ventricle heart model and 0D-closed-loop circulation model based on CircAdapt application. The research work [18] presented a model that described blood flow under aortic coarctation; the aortic arch itself was considered as a three-dimensional area whereas all the other vessels were de-

scribed with 0D and 1D models. If we want to create models that describe complex hydrodynamics and movements of the aortic valve leaflets, we should rely on an approach that involves interaction between a fluid and a solid body (fluid-solid interaction or FSI) [19, 20]. Two-dimensional (2D) FSI studies have certain limitations due to the aortic valve being highly turbulent. These 2D-models should be adapted to realistic 3D-model geometry [21, 22].

A challenge that doctors often have to face is related to the necessity to objectify a surgery to treat the aorta coarctation and to estimate impacts exerted on blood flow by properties of a shunt and a place where it is installed in order to secure proper lung development in children with congenital heart diseases. To solve this, it is advisable to create a patient-specific blood flow model at several scale levels. The previous stage in our research involved developing a conceptual 0D-3D scheme of systemic circulation in newborns with the modified Blalock – Taussig shunt (Figure 1); we considered the results of 0D-model in detail [23]. The 0D-model of systemic circulation is created by using the analogy between the blood flow in vessels and the flow of current through an electric circuit. A shunted section of the aorta and pulmonary artery is replaced with a 3D-model with two-way fluid-solid interaction (FSI). A section in a vessel with the aortic valve is examined in a separate 3D-model. The present study concentrates on algorithms for coupling developed models of different levels and some results of 3D-modeling that make it possible to predict whether shunting is effective as well as risks of complication after surgery.

**In this study**, we aimed to develop a coupled 0D-3D model of blood flow in newborns to predict risks of complications after surgery.

**Materials and methods.** The mathematical statement of the 0D task includes several tens of differential and algebraic equations. We applied Runge – Kutta 4<sup>th</sup> order method to find a numeric solution to them [23].

Geometry of the 3D-aortic valve model was created by using real CT-scans of a patient (Figure 2). The scans were transformed into a

three-dimensional solid-state model with In-Vesalius software. A computational mesh was created with Meshmixer software package. The fluid equations were solved by using CFD FLUENT software package; we applied Navier – Stokes equations and Continuity equations for an incompressible and homogeneous fluid. Any impacts exerted by gravity or heat

transfer between blood and the aortic valve were neglected in the models since their influence on the leaflet deformity was very slight. We applied the  $k-\epsilon$  model [24] to simulate turbulence in the aortic valve. The aorta and valve leaflets were modeled as hyper-elastic and the elasticity law was set with the Ogden 1<sup>st</sup> order hyper-elastic model [24].

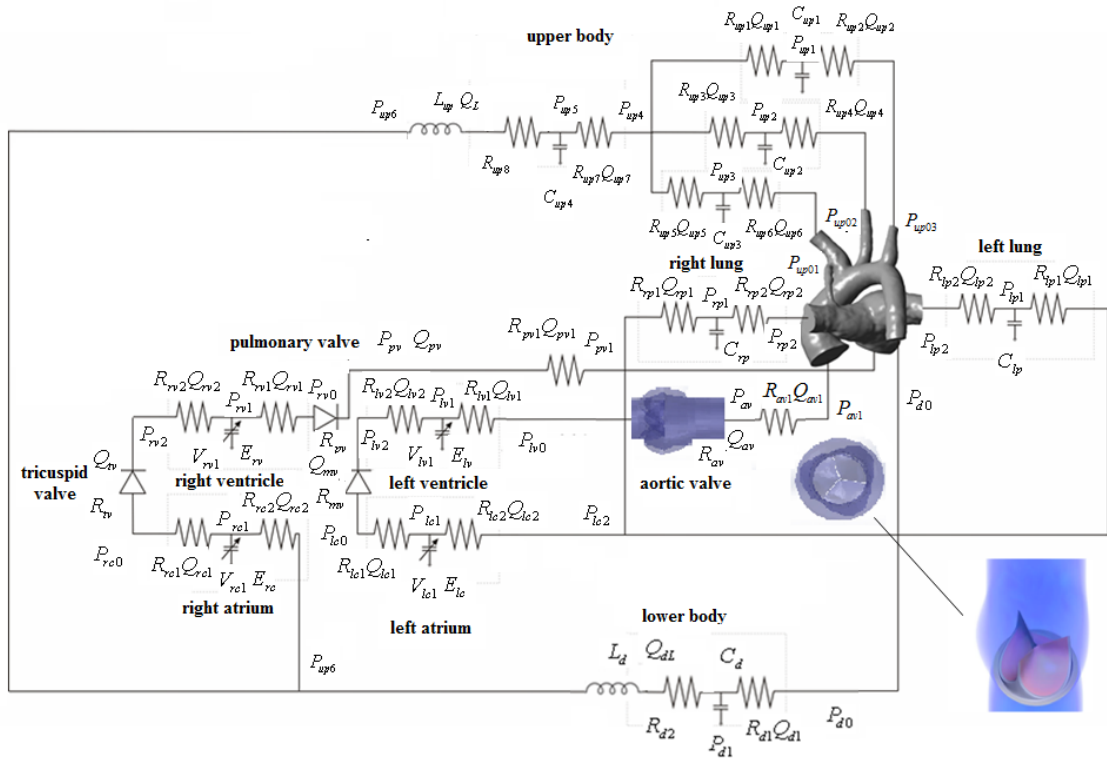


Figure 1. The conceptual scheme of systemic circulation [23]

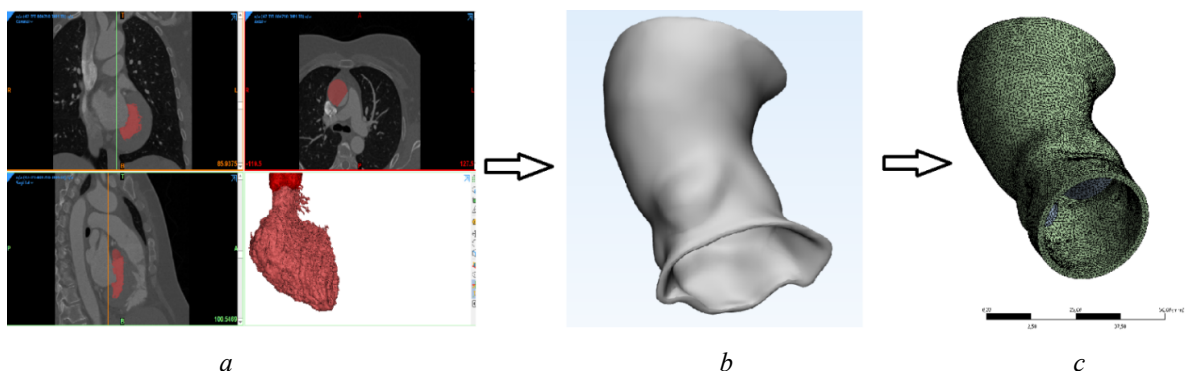


Figure 2. *a* shows CT scans of a patient’s chest; *b* is a solid-state model; *c* is a created computational mesh

A similar approach was used to simulate a three-dimensional flow in the shunted section of the aorta and pulmonary artery.

The algorithm for coupling models of different levels relies on meeting the condition that pressures and volume blood flows are equal at the interaction boundary [25]. Let us consider stages in the iteration algorithm: 1) blood flows and pressures that were identified at the initialization stage are fed into the 3D-model for solution; 2) pressures at the inlet and blood flows at the outlet are calculated within the stationary task in the 3D-model; 3) values calculated at the stage 2 are again returned into the 0D-model as boundary conditions to solve the equations and determine blood flows at the inlet to the aorta and pulmonary artery and pressures at the outlets; 4) convergence conditions at the boundaries are checked:

$$\begin{aligned} |P_{(i)}^{(0)(k)} - P_{(i)}^{(0)(k-1)}| < \delta P_{(i)}; \\ |Q_{(i)}^{(0)(k)} - Q_{(i)}^{(0)(k-1)}| < \delta Q_{(i)}, \end{aligned} \quad (1)$$

where  $P_{(i)}^{(0)(k)}$  is the pressure at the  $i$ -th boundary at the zero moment at the  $k$ -th iteration ( $k = 1$  for the 1<sup>st</sup> iteration);

$Q_{(i)}^{(0)(k)}$  is the volume flow at the  $i$ -th boundary at the zero moment at the  $k$ -th iteration;

$\delta P_{(i)}$ ,  $\delta Q_{(i)}$  are values of convergence criteria.

If the criteria (1) are met, we consider that the solution has been found at the zero step and we can move to the next time step. Otherwise, the values  $Q_{(i)}^{(0)(k)}$  at the inlets and  $P_{(i)}^{(0)(k)}$  at the outlets are again fed into the 3D-model, and the algorithm is repeated starting from the stage 2.

The algorithm for identifying patient-specific parameters is based on finding such a solution to the optimization task that would provide the periodicity of the solution on blood flow and pressure at any point in the 0D-model. We are planning to consider this algorithm in detail in our next articles.

**Results and discussion.** A time-dependent velocity at the inlet to the aortic valve was set as a sinusoid with the maximum flow velocity being 0.4 m/sec at peak systole. Shear strain velocity exceeded  $50 \text{ sec}^{-1}$  for large arteries and blood viscosity was almost constant due to high shear velocity [26]. Therefore, blood was considered a Newtonian fluid with constant density being  $1050 \text{ kg/m}^3$  and dynamic viscosity being  $0.0035 \text{ Pa}\cdot\text{sec}$  [20].

Computational experiments made it possible to analyze several properties of flow with different individual geometry of the aorta and valve. Figure 3 shows the most eligible computational mesh considering better convergence for a case when peak values of flow properties are observed. Such values are typical for pathological states.

Figure 4a shows how velocities are distributed in the aorta. The peak velocity reaches 1.874 m/sec at the narrowest sections and this is by 4.68 times higher than flow velocity at the inlet to the aorta. Turbulence zones are also visible. The highest wall shear stress value is at the valve leaflets from the incoming flow (Figure 4b). The highest value is 209.4 Pa whereas was shear stress at the aorta wall reaches only 15 Pa. Figure 4B shows shifts against the initial state (at the zero moment) up to its position after computations. The Figure 4d has sections painted red that means they are the most susceptible to elastic deformations. They are interleaflet triangles. The results show shifts of the valve leaflets and aorta walls. We can also see blood turbulences in the area close to the semilunar cusps. These observable wall shear stresses can be considered risk factors that can induce calcification of the valve leaflet and other valve diseases.

A model where the shunt was in the central position was taken as a computational area within the 3D “aorta – shunt – pulmonary artery” system. The solution to the task made it possible to identify distribution of some hemodynamic parameters that had medical significance. These parameters were velocity properties of blood flow, pressure on vessel

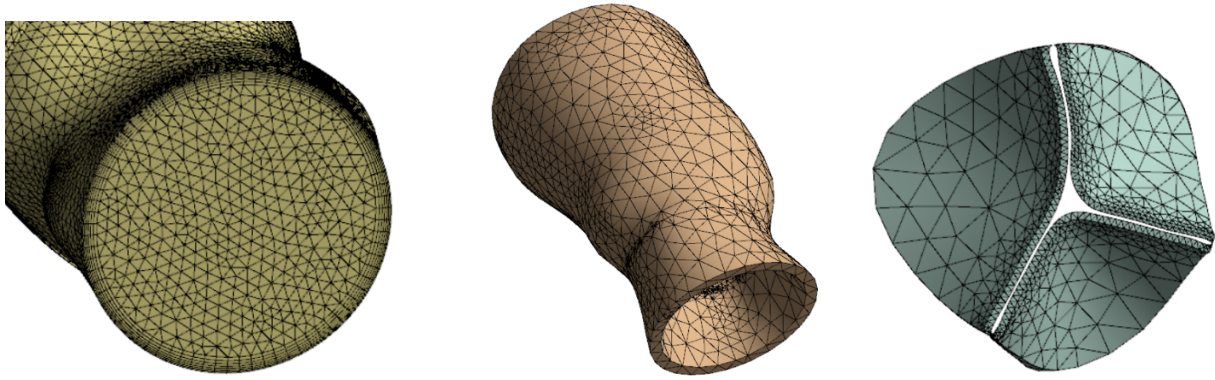


Figure 3. Visual images of computational meshes (from left to right: aorta cross section, aorta wall, valve leaflet)

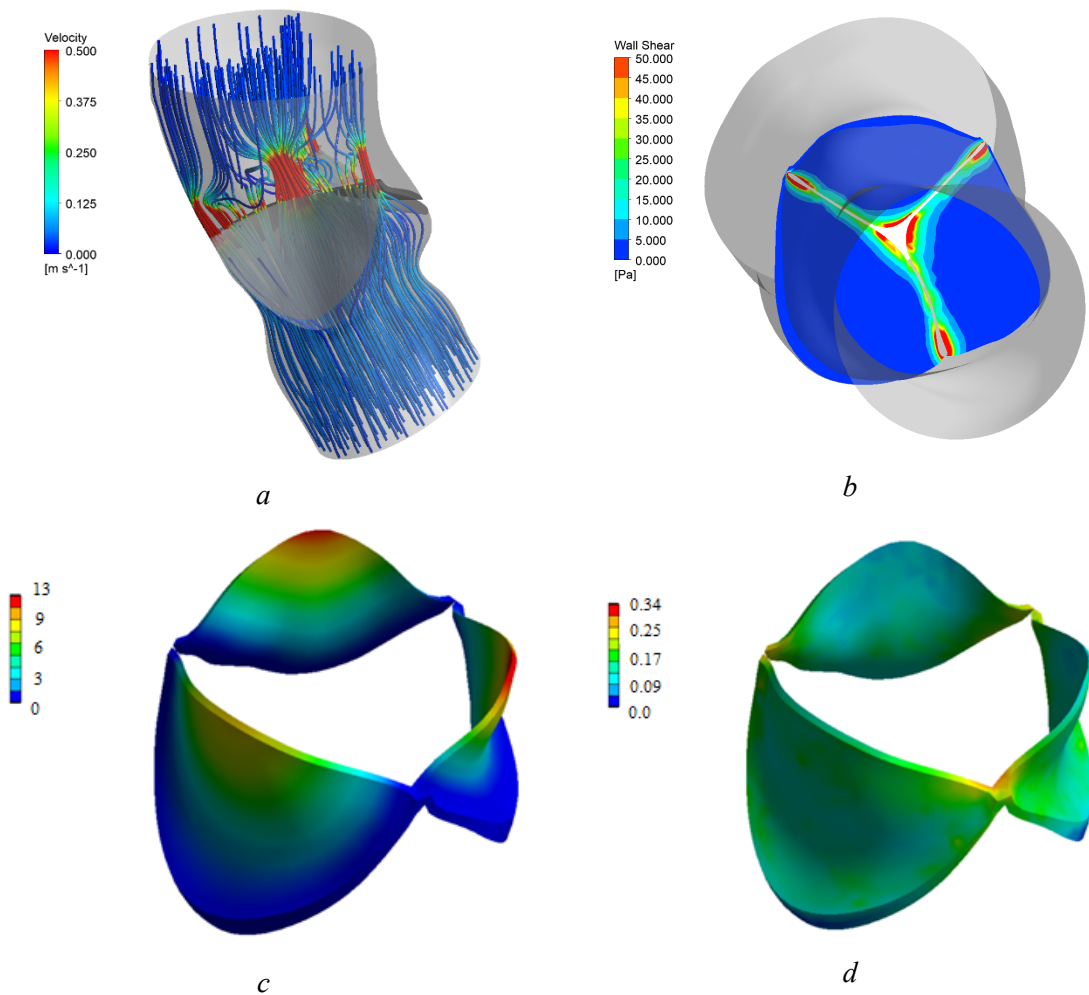


Figure 4. Distribution of flow properties in the aorta: *a* is for velocities; *b*, wall shear stresses; *c*, shifts of the aortic valve leaflets; *d*, equivalent elastic deformations of the aortic valve leaflets

walls, wall shear stresses, and wall shear stresses averaged over the cardiac cycle. The results were obtained at a moment that corresponded to the maximum value of the volume

blood flow  $t = 0.125$  sec. The velocity distribution under using 0D-boundary conditions is well in line with the data available in other research works [25] (Figure 5a) in spite of dif-

ferent model geometries. The maximum velocities are observed in the area where the shunt and the artery are joined and in the shunt itself; the lowest ones are detected in the pulmonary artery area. The maximum blood flow values are detected in the shunt area (values vary within 6 m/sec). As for shear stress distribution, it is noteworthy that the results are consistent with those available in literature [25] (Figure 5b) both qualitatively and quantitatively. The maximum values are detected in the area where the aorta branches and in the shunt and vary within the limit of 100 Pa. The lowest values are mostly observed in the pulmonary artery and the ascending and descending part of the aorta. When comparing the results, we should note that there were also some

differences detected in the modeling. The velocity distribution is different from those described in literature where the maximum velocities reached only 3.6 m/sec [27]. The same goes for distribution of shear stresses and pressures averaged over the cardiac cycle. The maximum shear stress values differ by more than twice: 40 Pa in the articles [27, 28] and 100 Pa as in the Figure 5b. The maximum pressure values also differ by 2 times: 13.89 kPa in the works [27, 28] and 26 kPa in our study (Figure 5c). The maximum values of shear stresses averaged over the cardiac cycle differ by more than 3 times: 45 Pa in the works [27, 28] and 150 Pa in the Figure 5d. These differences arise solely due to different approaches to simulating blood flow, namely,

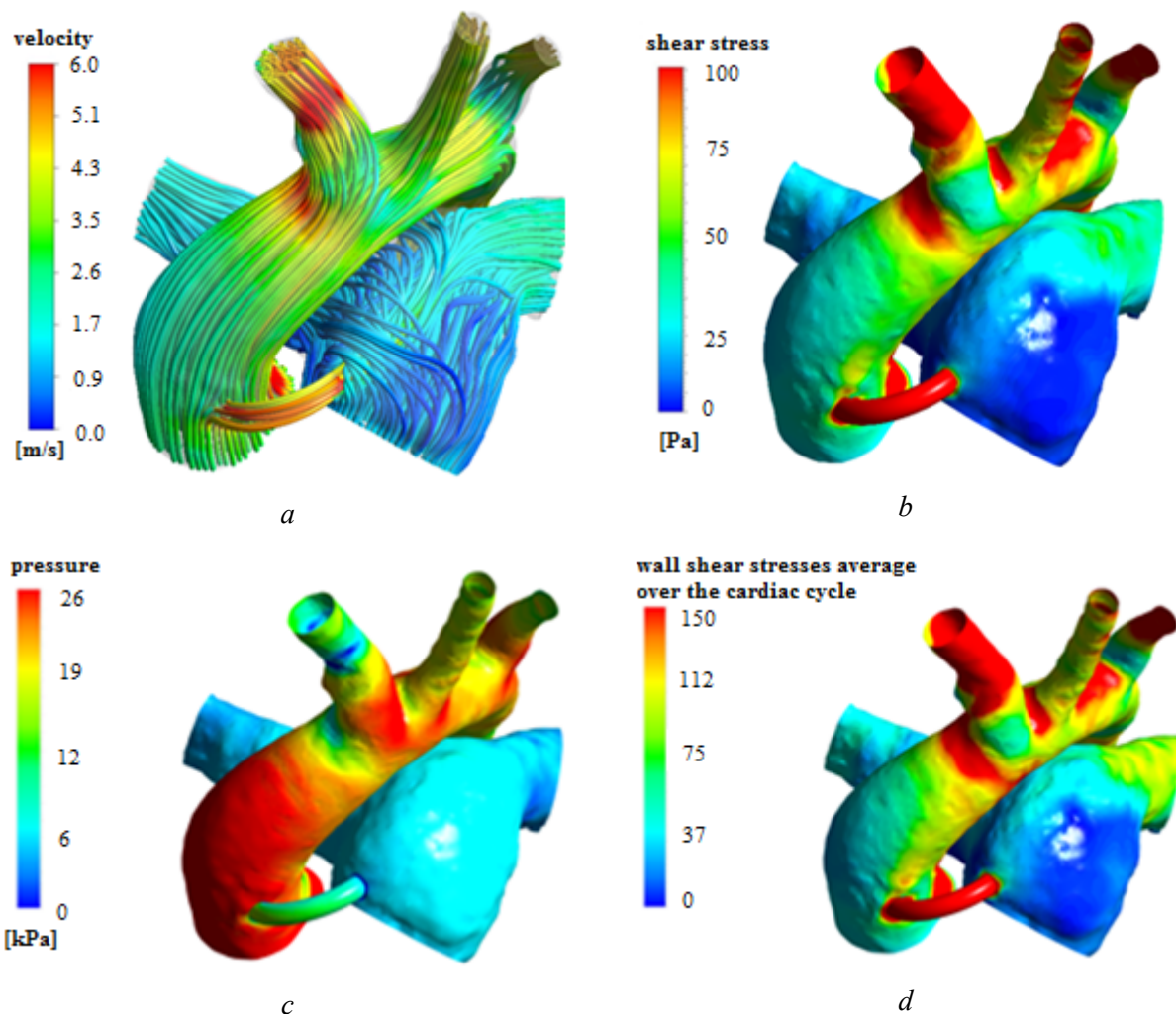


Figure 5. Distribution of blood properties in the 3D “aorta – shunt – pulmonary artery” system: *a* is velocity; *b*, shear stress; *c*, pressure; *d*, wall shear stresses average over the cardiac cycle



different boundary conditions. In the work [27], some average velocity profiles are set at the inlet and some constant pressures are set at the outlets. In our study, these boundary conditions are determined by finding a joint solution to the 0D-3D systemic circulation model. A result obtained for a specific patient can be interpreted as a high risk of complications developing in the middle term when the shunt is placed in the central position.

**Conclusion.** We have developed a coupled 0D-3D model of blood flow in newborns to predict risks of complications after surgery. The results obtained by 0D-modeling make it possible to predict how blood flow would be distributed in varied body parts and to estimate changes in blood flow into the lungs after shunting. On the other hand, three-dimensional tasking to simulate blood flow in the aortic valve and “aorta – shunt – pulmonary artery” system allows predicting significant hemodynamic parameters with spatial distribution thereby making it possible to visualize the most critical points.

The results obtained by patient-specific modeling have been shown to establish considerably different hemodynamic properties when coupled models are used. This empha-

sizes the importance of using patient-specific model parameters. The developed approaches, first of all, can be useful for decision-making in surgical practices to predict risks of complications under different variants of surgery. At present, this task might be too difficult to solve due to huge computational powers necessary to accomplish the required calculations.

In future we plan to develop an algorithm for selecting optimal shunting parameters such as a place where a shunt would be located and its size by performing a relevant numeric experiment. It is also advisable to develop approaches that could be used to assess risks of shunt thrombosis. We plan to develop the model so that it covers saturation and oxygen exchange. This is necessary for assessing whether oxygen supply to the lungs is adequate.

**Funding.** The research was accomplished due to financial support provided by the Russian Foundation for Basic Research and Perm region within the research project No. 20-41-596005.

**Competing interests.** The authors declare no competing interests.

## References

1. Driscoll D.J., Michels V.V., Gersony W.M., Hayes C.J., Keane J.F., Kidd L., Pieroni D.R., Rings L.J. [et al.]. Occurrence risk for congenital heart defects in relatives of patients with aortic stenosis, pulmonary stenosis, or ventricular septal defect. *Circulation*, 1993, vol. 87, suppl. 2, pp. II14–II20.
2. Moulton A.L., Brenner J.I., Ringel R., Nordenberg A., Berman M.A., Ali S., Burns J. Classic versus modified Blalock-Taussig shunts in neonates and infants. *Circulation*, 1985, vol. 72, no. 3, pt 2, pp. II35–II44.
3. De Leval M.R., McKay R., Jones M., Stark J., Macartney F.J. Modified Blalock-Taussig shunt. Use of subclavian artery orifice as flow regulator in prosthetic systemic-pulmonary artery shunts. *J. Thorac. Cardiovasc. Surg.*, 1981, vol. 81, no. 1, pp. 112–119.
4. Myers J.W., Ghanayem N.S., Cao Y., Simpson P., Trapp K., Mitchell M.E., Tweddell J.S., Woods R.K. Outcomes of systemic to pulmonary artery shunts in patients weighing less than 3 kg: analysis of shunt type, size, and surgical approach. *J. Thorac. Cardiovasc. Surg.*, 2014, vol. 147, no. 2, pp. 672–677. DOI: 10.1016/j.jtcvs.2013.09.055
5. Ahmad U., Fatimi S.H., Naqvi I., Atiq M., Moizuddin S.S., Sheikh K.B., Shahbuddin S., Naseem T.M., Javed M.A. Modified Blalock-Taussig shunt: immediate and short-term follow-up results in neonates. *Heart Lung Circ.*, 2008, vol. 17, no. 1, pp. 54–58. DOI: 10.1016/j.hlc.2007.06.003
6. Dirks V., Prêtre R., Knirsch W., Valsangiacomo Buechel E.R., Seifert B., Schweiger M., Hübler M., Dave H. Modified Blalock Taussig shunt: a not-so-simple palliative procedure. *Eur. J. Cardiothorac. Surg.*, 2013, vol. 44, no. 6, pp. 1096–1102. DOI: 10.1093/ejcts/ezt172
7. Geddicke M., Morgan G., Parry A., Martin R., Tulloh R. Risk factors for acute shunt blockage in children after modified Blalock-Taussig shunt operations. *Heart Vessels*, 2010, vol. 25, no. 5, pp. 405–409. DOI: 10.1007/s00380-009-1219-1

8. Sun L., Chandra S., Sucusky P. Ex vivo evidence for the contribution of hemodynamic shear stress abnormalities to the early pathogenesis of calcific bicuspid aortic valve disease. *PLoS One*, 2012, vol. 7, no. 10, pp. e48843. DOI: 10.1371/journal.pone.0048843
9. Ruiz J.L., Hutcheson J.D., Aikawa E. Cardiovascular calcification: current controversies and novel concepts. *Cardiovasc. Pathol.*, 2015, vol. 24, no. 4, pp. 207–212. DOI: 10.1016/j.carpath.2015.03.002
10. Maganti K., Rigolin V.H., Sarano M.E., Bonow R.O. Valvular heart disease: diagnosis and management. *Mayo Clin. Proc.*, 2010, vol. 85, no. 5, pp. 483–500. DOI: 10.4065/mcp.2009.0706
11. Votta E., Le T.B., Stevanella M., Fusini L., Caiani E.G., Redaelli A., Sotiropoulos F. Toward patient-specific simulations of cardiac valves: state-of-the-art and future directions. *J. Biomech.*, 2013, vol. 46, no. 2, pp. 217–228. DOI: 10.1016/j.jbiomech.2012.10.026
12. Ceballos A., Prather R., Divo E., Kassab A.J., DeCampi W.M. Patient-Specific Multi-Scale Model Analysis of Hemodynamics Following the Hybrid Norwood Procedure for Hypoplastic Left Heart Syndrome: Effects of Reverse Blalock-Taussig Shunt Diameter. *Cardiovasc. Eng. Technol.*, 2019, vol. 10, no. 1, pp. 136–154. DOI: 10.1007/s13239-018-00396-w
13. Corsini C., Baker C., Kung E., Schievano S., Arbia G., Baretta A., Biglino G., Migliavacca F. [et al.]. An integrated approach to patient-specific predictive modeling for single ventricle heart palliation. *Comput. Methods Biomech. Biomed. Engin.*, 2014, vol. 17, no. 14, pp. 1572–1589. DOI: 10.1080/10255842.2012.758254
14. Chi Z., Beile L., Deyu L., Yubo F. Application of multiscale coupling models in the numerical study of circulation system. *Medicine in Novel Technology and Devices*, 2022, vol. 14, pp. 100117. DOI: 10.1016/j.medntd.2022.100117
15. Dobroserdova T., Olshanskii M., Simakov S. Multiscale coupling of compliant and rigid walls blood flow models. *International journal for numerical methods in fluids*, 2016, vol. 82, no. 12, pp. 799–817. DOI: 10.1002/flid.4241
16. Shavik S.M., Tossas-Betancourt C., Figueroa C.A., Baek S., Lee L.C. Multiscale Modeling Framework of Ventricular-Arterial Bi-directional Interactions in the Cardiopulmonary Circulation. *Front. Physiol.*, 2020, vol. 11, pp. 2. DOI: 10.3389/fphys.2020.00002
17. Augustin C.M., Gsell M.A.F., Karabelas E., Willemen E., Prinzen F.W., Lumens J., Vigmond E.J., Plank G. A computationally efficient physiologically comprehensive 3D–0D closed-loop model of the heart and circulation. *Comput. Methods Appl. Mech. Eng.*, 2021, vol. 386, pp. 114092. DOI: 10.1016/j.cma.2021.114092
18. Mercuri M., Wustmann K., von Tengg-Koblighk H., Göksu C., Hose D.R., Narracott A. Subject-specific simulation for non-invasive assessment of aortic coarctation: Towards a translational approach. *Med. Eng. Phys.*, 2020, vol. 77, pp. 69–79. DOI: 10.1016/j.medengphy.2019.12.003
19. Mao W., Caballero A., McKay R., Primiano C., Sun W. Fully-coupled fluid-structure interaction simulation of the aortic and mitral valves in a realistic 3D left ventricle model. *PLoS One*, 2017, vol. 12, no. 9, pp. e0184729. DOI: 10.1371/journal.pone.0184729
20. Spühler J.H., Jansson J., Jansson N., Hoffman J. 3D Fluid-Structure Interaction Simulation of Aortic Valves Using a Unified Continuum ALE FEM Model. *Front. Physiol.*, 2018, vol. 9, pp. 363. DOI: 10.3389/fphys.2018.00363
21. Hsu M.C., Kamensky D., Bazilevs Y., Sacks M.S., Hughes T.J. Fluid-structure interaction analysis of bioprosthetic heart valves: Significance of arterial wall deformation. *Comput. Mech.*, 2014, vol. 54, no. 4, pp. 1055–1071. DOI: 10.1007/s00466-014-1059-4
22. Luraghi G., Wu W., De Gaetano F., Rodriguez Matas J.F., Moggridge G.D., Serrani M., Stasiak J., Costantino M.L., Migliavacca F. Evaluation of an aortic valve prosthesis: Fluid-structure interaction or structural simulation? *J. Biomech.*, 2017, vol. 58, pp. 45–51. DOI: 10.1016/j.jbiomech.2017.04.004
23. Kamaltdinov M.R., Kuchumov A.G. Application of a mathematical model of systemic circulation for determination of blood flow parameters after modified Blalock-Taussig shunt operation in newborns. *Russian Journal of Biomechanics*, 2021, vol. 25, no. 3, pp. 268–284. DOI: 10.15593/RJBiomech/2021.3.07
24. Amindari A., Saltik L., Kirkkopru K., Yacoub M., Yalcin H.C. Assessment of calcified aortic valve leaflet deformations and blood flow dynamics using fluid-structure interaction modeling. *Inform. Med. Unlocked*, 2017, vol. 9, pp. 191–199. DOI: 10.1016/j.imu.2017.09.001



25. Zhao X., Liu Y., Ding J., Ren X., Bai F., Zhang M. Hemodynamic effects of the anastomoses in the modified Blalock–Taussig shunt: a numerical study using a 0D/3D coupling method. *J. Mech. Med. Biol.*, 2015, vol. 15, no. 01, pp. 1550017. DOI: 10.1142/S0219519415500177
26. Young D.F. Fluid mechanics of arterial stenosis. *J. Biomech. Eng.*, 1979, vol. 101, pp. 157–175. DOI: 10.1115/1.3426241
27. Kuchumov A.G., Khairulin A.R., Biyanov A.N., Porodikov A.A., Arutyunyan V.B., Sinel'nikov Yu.S. Effectiveness of Blalock-Taussig shunt performance in the congenital heart disease children. *Russian Journal of Biomechanics*, 2020, vol. 24, no. 1, pp. 65–83. DOI: 10.15593/RJBiomech/2020.1.08
28. Kuchumov A.G., Khairulin A., Shmurak M., Porodikov A., Merzlyakov A. The Effects of the Mechanical Properties of Vascular Grafts and an Anisotropic Hyperelastic Aortic Model on Local Hemodynamics during Modified Blalock-Taussig Shunt Operation, Assessed Using FSI Simulation. *Materials (Basel)*, 2022, vol. 15, no. 8, pp. 2719. DOI: 10.3390/ma15082719

*Kuchumov A.G., Kamaltdinov M.R., Khairulin A.R., Kochergin M.V., Shmurak M.I. Patient-specific 0D–3D modeling of blood flow in newborns to predict risks of complications after surgery. Health Risk Analysis, 2022, no. 4, pp. 159–167. DOI: 10.21668/health.risk/2022.4.15.eng*

Received: 23.08.2022

Approved: 03.10.2022

Accepted for publication: 18.12.2022